Colloid Polym Sci (2007) 285:1129–1137
DOI 10.1007/s00396-007-1665-1

ORIGINAL CONTRIBUTION

Association behavior of one-end hydrophobically modified poly[N^5-(2-hydroxyethyl) L-glutamine] in water/ethylene glycol mixed solvent

Katsuhiro Inomata · Reina Doi · Erina Yamada · Hideki Sugimoto · Eiji Nakanishi

Received: 26 January 2007 / Accepted: 22 February 2007 / Published online: 16 March 2007

Abstract Amphiphilic polymers C*n*-PHEG consisting of water-soluble poly[N^5-2-(hydroxyethyl) L-glutamine] (PHEG) and hydrophobic alkyl chain (carbon number n= 12, 14, 16, or 18) attached at the PHEG terminal was prepared, and association behavior and structure of associate for C*n*-PHEG in selective solvent (water/ethylene glycol mixed solvent) have been investigated. α-Helix content of PHEG block for all the polymers increased with weight fraction of ethylene glycol in the mixed solvent (W_{EG}). By light scattering measurements, formation of a small micelle was suggested for C14-, C16-, and C18-PHEG when W_{EG}=0. With the increase in W_{EG}, appearance of a larger associate was revealed for C16- and C18-PHEG. Evaluated molecular weight and radius of gyration suggested that the micelle is star-like sphere when W_{EG}=0 and worm-like cylinder when W_{EG}=0.7. C12-PHEG did not demonstrate any distinct micellization behavior because of the weak hydrophobicity of C12 chain.

Keywords Poly[N^5-(2-hydroxyethyl) L-glutamine] · Micelle · Association behavior · Amphiphilic polymers · Light scattering

Introduction

Nonionic surfactant consisting of a water-soluble poly (ethylene glycol) (PEG) and a hydrophobic alkyl chain, C*i*E*j* where *i* and *j* are numbers of carbon atom in the alkyl chain and repeating unit of PEG block, respectively, is know to form micelles with various shape in dilute aqueous solution via association of the hydrophobic alkyl chain [1–12]. Recently, Einaga et al. [5–10] reported precise characterization of the worm-like micelles formed by association of C*i*E*j* having relatively short PEG chain by means of light scattering technique and based on a scattering theory for worm-like micelles proposed by Sato [13]. On the other hand, formation of spherical micelle has been reported for C12E25 [11, 12], which has longer hydrophilic PEG chains. These results suggest that the micellar structure of C*i*E*j* will be influenced by chain length of the hydrophilic block and/or association strength of the hydrophobic group.

In our previous report, association behavior of both-ends hydrophobically modified water-soluble polypeptide was investigated [14]. This associative polymer, C12-PHEG-C12, consisted of nonionic water-soluble polypeptide poly [N^5-2-(hydroxyethyl) L-glutamine] (PHEG) and dodecyl chains (C12) bonded at both chain ends of PHEG. Water/ethylene glycol (EG) mixed solvent was used as a selective solvent for the middle PHEG chain. PHEG is know to exhibit helix-coil transition in water/alcohol mixed solvent with the change of the solvent composition [15–19], i.e., PHEG is in random coil state in pure water, and its α-helix content increases with the increase in alcoholic EG content in the mixed solvent (weight fraction of EG was designated as W_{EG}). In pure water, C12-PHEG-C12, having molecular weight of 9,700, was suggested to form isolated small micelle by the association of the terminal C12 chains. With the increase in EG content in the solvent and α-helix content of PHEG block, the size of the associate increased drastically. This result was explained by the conformation change of PHEG with W_{EG}. In the small micelle, the middle

K. Inomata (✉) · R. Doi · E. Yamada · H. Sugimoto · E. Nakanishi
Department of Materials Science and Engineering,
Nagoya Institute of Technology,
Gokiso-cho, Showa-ku,
Nagoya 466-8555, Japan
e-mail: inomata.katsuhiro@nitech.ac.jp

PHEG was in flexible random coil state and taking a loop conformation. With the increase in the α-helix content, taking the loop conformation became difficult because of the increase in chain rigidity. Thus, the large associate formed in higher W_{EG} solution was considered to be a microgel-like aggregate containing many C12 cores connected by PHEG in bridge conformation.

In this study, we have prepared one-end hydrophobically modified PHEG, C*n*-PHEG, in which an alkyl chain is attached at one terminal of PHEG block where the number of carbon atoms *n* is 12, 14, 16, and 18 (Fig. 1). In these polymers, PHEG blocks have almost similar molecular weight. As the selective solvent for PHEG block, water/EG was also used. Systematic analyses of light scattering, circular dichroism (CD), and fluorescence spectroscopy measurements for dilute solutions of these polymers with varying EG content have been investigated. From the evaluated results, influences of the association strength of the hydrophobic alkyl chain and conformation of the hydrophilic PHEG chain on the association behavior of C*n*-PHEG will be discussed.

Because of biocompatible and biodegradable nature of polypeptides, association behavior of various block and graft copolymers containing polypeptide blocks have been investigated recently for the purpose of preparing surfactants, nanoparticles, micelle drug carriers, and so on [20–26]. Effects of polypeptide's conformation on the association of the copolymers were also studied [19, 21, 23]. The results obtained in the present work will provide a useful information for investigating a stimuli-responsible biomimetic material, which can control a self-assembled nanoscale structure [25].

Experimental section

Materials

Butylamine (C4-NH_2), dodecylamine (C12-NH_2), 2-aminoethanol, 2-hydroxypyridine, and EG were fractionally distilled before use. Tetradecylamine (C14-NH_2), hexadecylamine (C16-NH_2), and octadecylamine (C18-NH_2) were purified by recrystallization from diethyl ether. *N*-carboxyanhydride (NCA) of γ-benzyl L-glutamate (BLG) was prepared by reacting BLG with triphosgene [27] and purified by recrystallization from tetrahydrofurane/petrorium ether. Distilled water was ion-exchanged before use.

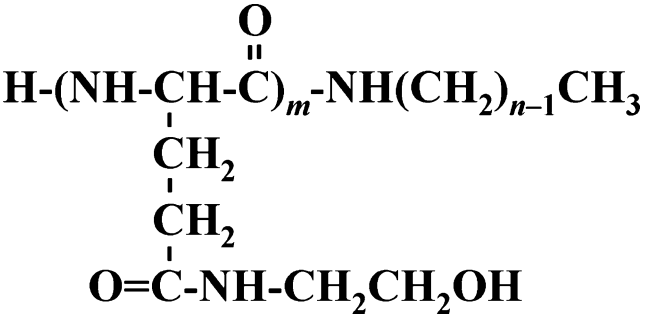

Fig. 1 Chemical structure of C*n*-PHEG

Synthesis of C*n*-PHEG

NCA of BLG was polymerized by using C*n*-NH_2 in dry dichloromethane at room temperature for 4 days. The solution was poured into cold methanol, and precipitates were filtered and washed with diethyl ether. The obtained C*n*-poly(γ-benzyl L-glutamate) (C*n*-PBLG) and 2-hydroxypyridine (fivefold molar) were dissolved in *N*,*N*-dimethylformamide (DMF), 20-fold molar amount of 2-aminoethanol was added, and side-chain exchanging reaction was performed for 24 h at 26 °C [14, 28]. The reaction solution was neutralized by acetic acid/methanol (1:1 in volume) and dialyzed against water by using cellulose membrane with nominal fractional molecular weight of 3,500. C*n*-PHEG was obtained after freeze-drying of aqueous polymer solution.

Measurements

^{1}H-NMR spectrum of C*n*-PHEG was recorded on an Avance200 (Bruker) with using dimethyl sulfoxide (DMSO)-d_6 as solvent. Size exclusion chromatography (SEC) chart was recorded on a SC-8020 (TOSO). Eluent solvent was DMF/LiBr (1 wt%), and standard polystyrene was used for molecular weight calibration.

CD measurements were performed on a J-820/805 (JASCO) using a quartz cell having a path length of 1 mm. Polymer concentration of the solution was ca. 5×10^{-4} g/ml, and solution temperature was maintained at 30 °C.

Fluorescence spectrum was measured on a RF-5300FC spectrophotofluorometer (Shimadzu) at room temperature to evaluate the critical micelle concentration (CMC) of C*n*-PHEG aqueous solution. 1-Anilino-8-naphthalen sulfonic acid magnesium salt (ANS-Mg, concentration 1.6×10^{-6} M) was used as fluorescence probe. An excitation wavelength of 350 nm was employed for the measurements.

Static and dynamic light scattering (SLS and DLS, respectively) was measured by a laboratory-made apparatus equipped with an ALV/SO-SIPD detector and an ALV-5000 correlator using He–Ne laser (wavelength λ_0=633 nm) as a light source [12, 29]. Sample solutions were optically purified by a Millipore filter of nominal pore size of 0.45 or 1.0 mm and transferred into optical tube, and the tube was flame-sealed under gentle vacuum. Details of the analysis have been described in the previous paper [14, 19]. Solution temperature was maintained at 30 °C during the

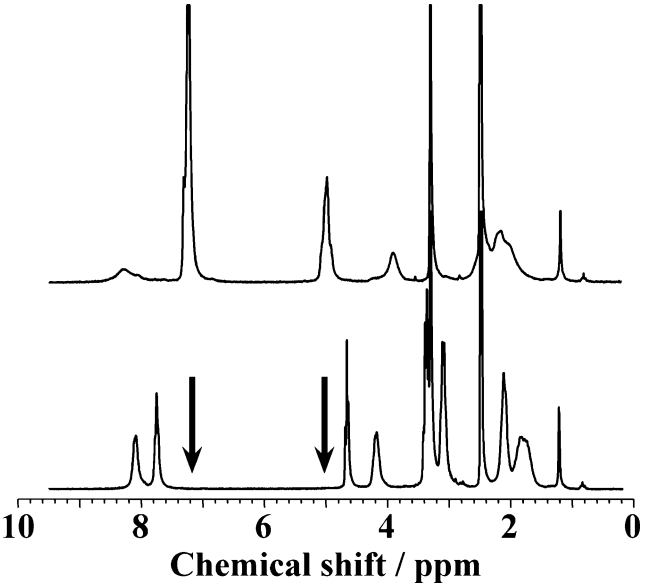

Fig. 2 ^{1}H NMR spectra for C14-PBLG (*upper*) and C14-PHEG (*lower*). DMSO-d_6 was used as solvent. As indicated by *arrows*, proton signals assigned as benzyl group disappeared in C*n*-PHEG

measurement. Conventional data analysis for SLS and DLS results by extrapolating to dilute limit was not applied because of a possibility of a concentration dependence of association behavior; therefore, evaluated weight-averaged molecular weight (M_w), radius of gyration (R_g), and hydrodynamic radius (R_h) are apparent ones at finite concentration [14, 19]. Refractive index increment d*n*/d*c* was measured by a differential refractometer RM-102 (Union Giken). Because of a small difference in the alkyl chain length, the following equation was used for all C*n*-PHEG samples.

$$\frac{dn}{dc}(\mathrm{ml/g}) = 0.1606 - 0.07845 W_{EG}. \quad (1)$$

In this equation, W_{EG} represents the weight fraction of EG for the water/EG mixed solvent; therefore, pure water and EG correspond to W_{EG}=0 and 1.0, respectively. Solvent viscosity was derived from the data reported by Tsierkezos and Molinou [30].

Sample solutions for CD, fluorescence spectroscopy, and light scattering measurements were prepared by dissolving the polymer in the mixed solvent, which was prepared at desired W_{EG} in advance, at room temperature. Because of the limitation of polymer solubility, solutions with W_{EG}> 0.7 could not be prepared for C14-, C16-, and C18-PHEG.

Results and discussion

Polymer characterization

Typical ^{1}H NMR spectra for C14-PHEG and its starting material, C14-PBLG, dissolved in DMSO-d_6 are shown in Fig. 2. After the side-chain exchanging aminolysis reaction, proton signals from –$CH_2C_6H_5$ benzyl group at 5.0 and 7.2 ppm disappeared, and newly appeared signals at 3.1, 3.4, 4.6, and 7.8 ppm can be assigned as protons in –$NHCH_2$ CH_2OH group (see Fig. 1). Number-averaged molecular weight (M_n) of the polymers and degree of polymerization (*m*) for PBLG or PHEG blocks were evaluated from peak area of signals from alkyl group and polypeptide group, and the obtained results are summarized in Table 1. From these results, the aminolysis reaction from C*n*-PBLG to C*n*-PHEG was found to proceed successfully without a main-chain cleavage. M_n for PHEG block in C12-, C14-, C16-, and C18-PHEG were in the range of 9,500–10,500. Because the alkyl chain length is short, the hydrophobicity of C4 group in C4-PHEG should be negligibly weak than the other C*n*-PHEGs. Molecular weight distribution index M_w/M_n for C*n*-PHEG evaluated from SEC results was ranged within 1.38–1.78. For C16-PHEG, however, M_w/M_n could not be determined because of its low solubility in the eluent solvent.

Conformation of PHEG

Typical examples of CD spectra for C*n*-PHEG in water/EG with various W_{EG} are shown in Fig. 3. When W_{EG}=0, the spectrum suggests that PHEG is in random-coil state, and

Table 1 Polymer characteristics

Sample code	m^a	M_n	M_w/M_n	CMC (g ml^{-1}) in aqueous solution
C18-PBLG	60	13,400	1.36	
C16-PBLG	56	12,500	2.06	
C14-PBLG	59	13,100	1.83	
C12-PBLG	61	13,500	1.43	
C4-PBLG	48	10,600	1.65	
C18-PHEG	59	10,400	1.38	1.6×10^{-4}
C16-PHEG	55	9,700	–	3.2×10^{-4}
C14-PHEG	61	10,700	1.72	1.2×10^{-3}
C12-PHEG	61	10,700	1.43	–
C4-PHEG	47	8,200	1.78	

[a] Degree of polymerization of PBLG or PHEG block

with the increase in W_{EG}, two minima at λ=208 and 222 nm can be clearly recognized. Observed mean residual ellipticity at λ=222 nm ($[\Theta]_{222}$) was used to evaluate the α-helix content f^{H} of PHEG block according to the next equation [14, 31].

$$f^{H} = \frac{[\Theta]_{222}\left(\mathrm{deg}\cdot\mathrm{cm}^2\cdot\mathrm{decimole}^{-1}\right)}{-40,000}. \quad (2)$$

Obtained f^{H} values are plotted against W_{EG} in Fig. 4. With the increase in W_{EG}, f^{H} value increased gradually, and this W_{EG} dependency was almost identical with that for C12-PHEG-C12 [14]. This figure indicates that the chain-length variation of the alkyl group attached at the PHEG terminal gives a little influence on PHEG conformation.

Fluorescence spectroscopy of C*n*-PHEG aqueous solution probed by ANS-Mg

Fluorescence spectroscopy measurements for C*n*-PHEG/water solution with various polymer concentrations probed by ANS-Mg were conducted, and some results are shown in Fig. 5. With the increase in polymer concentration *c*, the fluorescence peak of ANS in C14-, C16-, and C18-PHEG systems shifted to shorter wavelength, and its intensity increased drastically (Fig. 5a–c). When ANS molecule shifts from hydrophilic circumstance to hydrophobic one, it

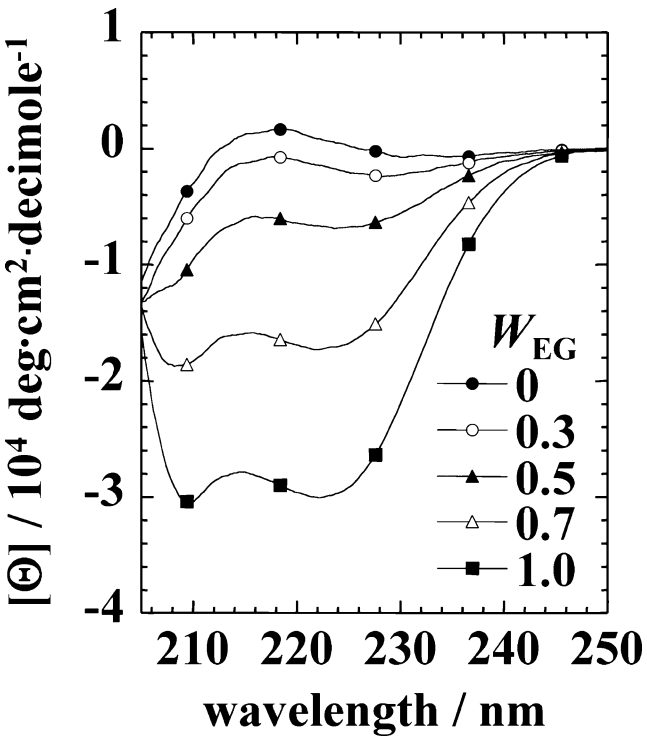

Fig. 3 CD spectra for C14-PHEG dissolved in water/EG mixed solvent. EG weight fraction, W_{EG}, is also indicated. Only limited experimental points are marked by the symbol

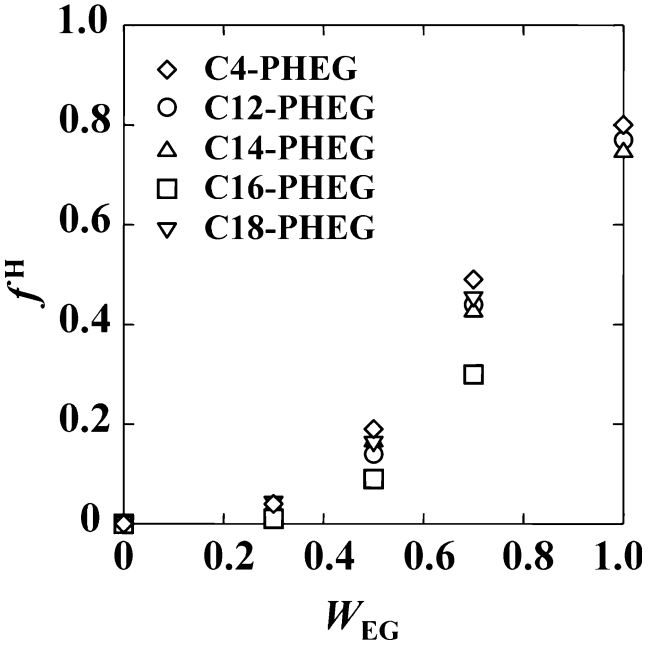

Fig. 4 Plots of α-helix content, f^{H}, for PHEG blocks against W_{EG}, evaluated from CD spectra for C*n*-PHEG

is reported that an intensity maximum of ANS fluorescence peak shifts to the shorter wavelength and its intensity increases [26]. Therefore, the spectra in Fig. 5a–c clearly indicate that ANS tends to be in a hydrophobic domain as a result of the association of alkyl chains. On the other hand, in C12-PHEG/water solutions, the peak shift and its intensity change were less clear as shown in Fig. 5d. This result suggests that the association behavior of C12-PHEG differs from that for other C*n*-PHEGs.

From the plots of peak wavelength against polymer concentration, CMC was evaluated and listed in the last column in Table 1, except C12-PHEG because of the reason above mentioned. These values indicate that C*n*-PHEG can easily form associated micelles with the alkyl chain length becomes longer.

Light scattering

C18-PHEG

DLS measurements for C18-PHEG solutions with various W_{EG} solvents having polymer concentration c=0.5 wt% were performed. Evaluated R_h distribution curves measured at scattering angle θ=90° are shown in Fig. 6a. In pure water (W_{EG}=0), a single distribution peak was observed around 10 nm. In W_{EG}=0.3 and 0.4 solutions, an additional peak having larger R_h was observed at around 30 nm. SLS measurements for these solutions were also conducted, and in Fig. 7, scattered light intensity measured at θ=45°, I(45°), are plotted against W_{EG}. The intensity of these solutions increased drastically with the increase in the relative peak

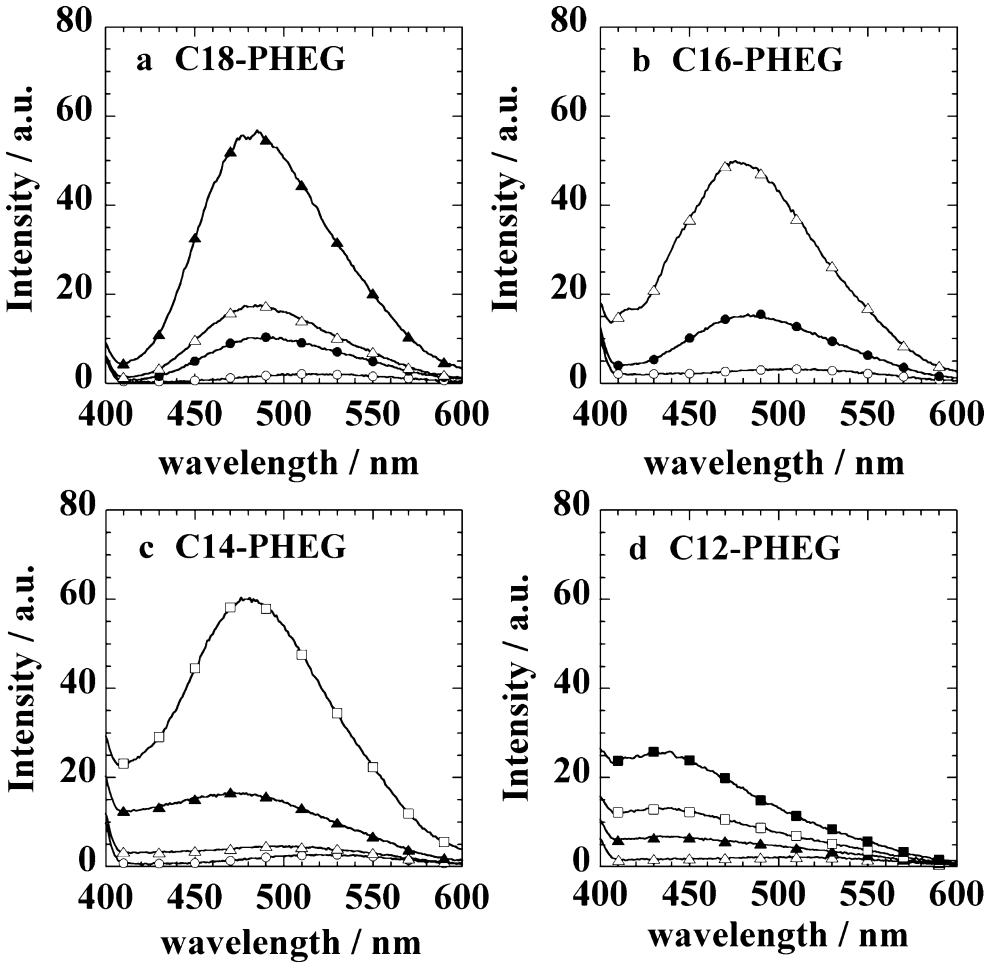

Fig. 5 Fluorescence spectra for aqueous solutions of **a** C18-PHEG, **b** C16-PHEG, **c** C14-PHEG, and **d** C12-PHEG. Polymer concentrations are 1×10^{-4} g/ml (○), 5×10^{-4} g/ml (●), 1×10^{-3} g/ml (△), 5×10^{-3} g/ml (▲), 1×10^{-2} g/ml (□), and 2×10^{-2} g/ml (■). Only limited experimental points are marked by the symbol

height for the larger particle in Fig. 6a. In the solution with W_{EG}=0.5, the evaluated distribution curve showed a broad peak around several hundred nanometers. It should be noted that in W_{EG}=0.5 solution, some precipitates were recognized a couple of days after the clearly dissolved solution was prepared. Therefore, the precipitates should be a result of a growth of the large particle with elapsing time. Right now, we cannot elucidate any reasons why the precipitates were

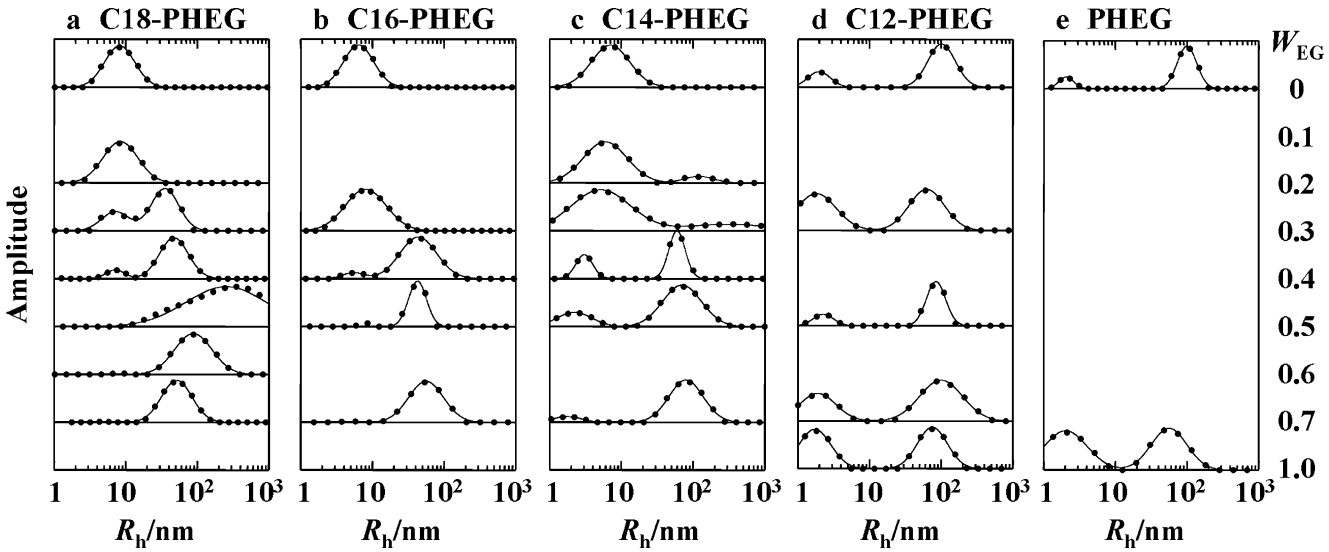

Fig. 6 R_h distribution curves measured at θ=90° for **a** C18-PHEG (c=0.5 wt%), **b** C16-PHEG (1.0 wt%), **c** C14-PHEG (2.0 wt%), **d** C12-PHEG (2.0 wt%), and **e** C4-PHEG (2.0 wt%) in various W_{EG} solutions as indicated

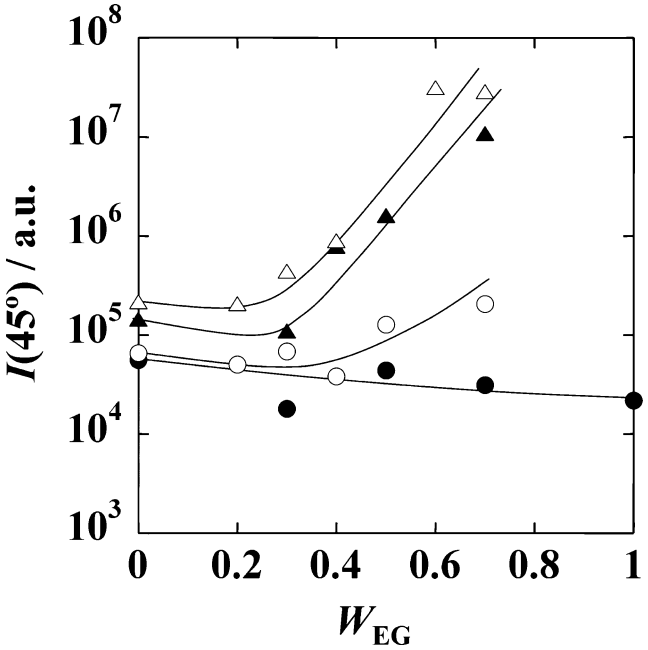

Fig. 7 Plots of scattered light intensity at θ=45°, I(45°), against W_{EG} for C18-PHEG (△), C16-PHEG (▲), C14-PHEG (○), and C12-PHEG (●) solutions

formed after the polymer was once dissolved completely. When W_{EG}=0.7, the R_h distribution curve revealed a peak at around several ten nanometers, which is almost identical to the size for the larger particle in W_{EG}=0.3 and 0.4 solutions.

R_h value at the top of the peak measured at various θ were plotted against square of scattering vector, q^2, where q is defined by $(4\pi n/\lambda_0)\sin(\theta/2)$ and n the refractive index of the solvent. Apparent R_h at a finite concentration, $R_{h,app}$, was derived from this plot by extrapolation to q^2=0, and in Table 2, these $R_{h,app}$ values for small (<10 nm) and large (>40 nm) particles are listed. From the SLS measurements, apparent values at finite concentration for molecular weight $M_{w,app}$, association number $N_{app}=M_{w,app}/M_n$, and radius of gyration $R_{g,app}$ were evaluated if the R_h distribution curve in Fig. 6a was unimodal, and the results are also listed in Table 2.

C16-PHEG

R_h distribution curves for C16-PHEG solutions with c= 1.0 wt% are indicated in Fig. 6b. There are some similarities between Fig. 6a and b; however, the precipitation observed in W_{EG}=0.5 solution of C18-PHEG was not recognized in C16-PHEG systems. When W_{EG}=0 and 0.3, the peak located around R_h~7 nm, and N_{app} was evaluated as 11–14, which was smaller than those for C18-PHEG/water. In the solution of W_{EG}=0.4, an additional peak was recognized around several ten nanometers, and the I(45°) was suddenly increase around this W_{EG} value, as shown in Fig. 7. Single distribution peak was again observed when W_{EG}=0.7. Evaluated $R_{h,app}$, $R_{g,app}$, $M_{w,app}$, and N_{app} by the same manner as C18-PHEG are listed in Table 2.

C14-PHEG

R_h distribution curves for C14-PHEG/water/EG solutions with c=2.0 wt% are shown in Fig. 6c. When W_{EG}=0, a single peak located around ~10 nm can be recognized as like the results for C18-PHEG and C16-PHEG. With the increase in W_{EG}, a peak at larger R_h region appeared, and its relative peak height against that for the smaller particle increased. However, the scattered light intensity was weak as indicated in Fig. 7, i.e., C18- and C16-PHEG solutions exhibited drastic increase in I(45°) with 10^2~10^3 times by W_{EG} change from 0.3 to 0.7, but in C14-PHEG, I(45°) increased only several times. In the R_h distribution curve, the peak for the smaller particle was still observed even in W_{EG}=0.7 solution. Usually, scattering light intensity depends on the particle size; therefore, this distribution curve indicates that the larger particle's fraction should be little. With the increase in W_{EG}, the peak of the smaller particle gradually shifted to the left, and when W_{EG}=0.7,

Table 2 Numerical results of light scattering measurements for C*n*-PHEG/water/EG solutions

Polymer	W_{EG}	$R_{h,app}$/nm		$R_{g,app}$[a] /nm	$M_{w,app}$ /g mol^{-1}	N_{app}
		Small	Large			
C18-PHEG	0	8		14	217,000	21
(c=0.5 wt%)	0.2	8		26	199,000	19
	0.3	8	46			
	0.4	8	48			
	0.5		355			
	0.6		125			
	0.7		53	60	24,700,000	2,380
C16-PHEG	0	7		13	137,000	14
(c=1.0 wt%)	0.3	7		11	111,000	11
	0.4	4	53			
	0.5		45			
	0.7		64	73	11,100,000	1,140
C14-PHEG	0	7		(24)	63,000	6
(c=2.0 wt%)	0.2	6	145			
	0.3	4	74			
	0.4	3	71			
	0.5	2	72			
	0.7	2	94			
C12-PHEG	0	2	112			
(c=2.0 wt%)	0.3	2	96			
	0.5	2	86			
	0.7	2	122			
	1.0	2	129			

[a] Result containing large experimental error is indicated in parenthesis.

$R_{h,app}$ was evaluated as 2 nm. This value is consistent with a predicted radius of gyration of an isolated molecularly dissolved C14-PHEG, $\left\langle R_g^2 \right\rangle^{1/2} = 3.1$ nm, calculated from the reported characteristic ratio $\left\langle r^2 \right\rangle = 6\left\langle R_g^2 \right\rangle = 6.6$ ml^2 [32], where $<r^2>$ the mean square end-to-end distance, m the degree of polymerization, and l the distance between successive α-carbon atom (=0.38 nm). From these results, it may be plausible that C14 chains were not strongly associated when EG content was higher, and the unassociated C14-PHEG chains dominantly existed with a few large particles. Decrease in the association strength of the alkyl chain with the increase in W_{EG} was also pointed out in C12-PHEG-C12 systems [14]. Because of the coexistence of two kinds of particle, the evaluation of $M_{w,app}$ and $R_{g,app}$ by the conventional way was not performed. In Table 2, $R_{h,app}$ values for all solutions and SLS results for W_{EG}=0 solution are indicated.

C12-PHEG

DLS results for C12-PHEG solutions with c=2.0 wt% are shown in Fig. 6d. The distribution curve suggests an existence of two relaxation modes with its size of ~100 and ~2 nm in all solutions of W_{EG}=0~1.0. As shown in Fig. 5d, the fluorescence spectrum suggests that C12 chains did not form hydrophobic cores in water even when c=2×10^{-2} g/ml. Relative height for the peak at ~100 and ~2 nm in Fig. 6d reveals that the amount of the larger particle should be a little as pointed out in C14-PHEG. Evaluated $R_{h,app}$ value for the smaller particle (see Table 2) was also close to the calculated $\left\langle R_g^2 \right\rangle^{1/2}$ for isolated C12-PHEG chain, and I(45°) was much weaker than the other polymer solutions (Fig. 7). Therefore, we can conclude that almost all C12-PHEG chains were molecularly dissolved in these solutions because the association strength of C12 attached at one terminal of hydrophilic PHEG with M_n~10,000 was too weak to associate in water/EG mixed solvents. Possible reason for the formation of the large particle is that a very small amount of the benzyl side chains remained after the aminolysis reaction from C12-PBLG to C12-PHEG, which could not be detected by ^{1}H NMR. These hydrophobic benzyl groups cause multiple association to form a micro-gel-like large aggregate, as suggested in our previous work for the both-ends hydrophobically modified PHEG [14]. It should be noted that similar $R_{h,app}$ distribution curves were also obtained for C4-PHEG solutions as shown in Fig. 6e, in which the terminal n-butyl (C4) chain should be too short to form associates.

As indicated in the pervious paper [14], C12-PHEG-C12, having M_n of 9,500, which is close to that for C12-PHEG, formed distinct micelles as evidenced by light scattering and fluorescence spectroscopy. Therefore, we can point out that molecular weight balance of the hydrophilic PHEG and hydrophobic Cn sensitively affects the association behavior of Cn-PHEG.

Structure of the associates

As shown in Fig. 6, some solutions exhibited unimodal R_h distribution with single peak, i.e., W_{EG}=0 for C14-PHEG, W_{EG}=0, 0.3, and 0.7 for C16-PHEG, and W_{EG}=0, 0.2, and 0.7 for C18-PHEG. In the solutions with $W_{EG}\leq$0.3, the smaller particle with $R_{h,app}$=7~8 nm can be recognized, and the larger particle with R_h=60~80 nm was observed when W_{EG}=0.7. These particles coexisted in other solutions. Recently, light scattering analysis for bimodal systems by combined use of DLS and SLS results has been reported [33, 34]; however, we did not adopt this procedure in this work. In this section, consideration about the structure of associates will be performed only for the unimodal solutions.

When W_{EG} is small, C14-, C16- and C18-PHEG formed small micelles, and their N_{app} was 6~21 and $R_{h,app}$ was 7~8 nm. As mentioned in "Introduction", amphiphilic polymers with hydrophilic PEG and hydrophobic alkyl chain, CiEj, were reported to form worm-like cylindrical micelles in aqueous solutions when PEG chain length is short (molecular weight is less than several hundred) [5–10]. If PEG chain length is longer, a star-like spherical micelles was proposed for C12E25 (PEG molecular weight is 1,200) [11, 12]. Therefore, in our samples having much longer hydrophilic chain (M_n~10,000), star-like micelle might be expected. If the associated Cn cores strongly reject solvent molecule, hydrophobic core radius (r_c) can be evaluated by using N_{app} with assuming density for Cn chain (ρ) by using the following equation:

$$\frac{N_{app}(14.0n+1.0)}{\rho N_A} = \frac{4}{3}\pi r_c^3. \quad (3)$$

In this equation, N_A is the Avogadro constant. In Table 3, the evaluated r_c values are listed. As mentioned above, the radius of gyration for PHEG in random coil state can be calculated by using its degree of polymerization. In Table 3, obtained values of $R_{mic} = 2\left\langle R_g^2 \right\rangle^{1/2} + r_c$ are listed, and these results show excellent consistency with the experimentally obtained $R_{h,app}$. Therefore, in these solutions, Cn-PHEG most plausibly forms star-like spherical micelles with Cn-associated core and well-dissolved PHEG corona.

When W_{EG}=0.7, C16-PHEG and C18-PHEG formed unimodal large particle, and its size was several ten nanometers. With considering the molecular geometry of Cn-PHEG, simple star-like spherical micelles in W_{EG}=0 solutions cannot satisfy these large sizes. Here, we assume that C16- and C18-PHEG form worm-like cylindrical micelles in W_{EG}=0.7 solution, like CiEj aqueous solution with $j\leq$8 [5–10]. Relationship between diameter d and

Table 3 Evaluated micellar geometries with assuming star-like spherical shape

Polymer	W_{EG}	r_c/nm	$2< R_g^2 >^{1/2}$/nm	R_{mic}/nm	$R_{h,app}$/nm
C18-PHEG	0	1.3	6.1	7.4	8
	0.2	1.4	6.1	7.5	8
C16-PHEG	0	1.2	5.9	7.1	7
	0.3	1.1	5.9	7.0	7
C14-PHEG	0	0.85	6.2	7.0	7

contour length L of the spherocylinder can be expressed as follows:

$$\frac{N_{app}(14.0n+1.0)}{\rho N_A} = \frac{4}{3}\pi\left(\frac{d}{2}\right)^3 + (L-d)\pi\left(\frac{d}{2}\right)^2. \quad (4)$$

L can be calculated if N_{app} and d are given. Under the assumption that the dimension of the worm-like micelle can be represented by considering only the Cn-associated core, R_g for the worm-like micelle can be calculated by the following equation using the above-evaluated L [35, 36]:

$$R_g^2 = P^2\left[\frac{L}{3P} - 1 + \frac{2P}{L} - \frac{2\{1-\exp(-L/P)\}}{(L/P)^2}\right]. \quad (5)$$

In this equation, P is the persistence length of the worm-like chain and was evaluated as to satisfy the observed $R_{g,app}$. The fitting process revealed that a possible data set of d, L, and P could be obtained when $d \leq 1.7$ nm for C16-PHEG and $d \leq 2.8$ nm for C18-PHEG. The worm-like chain becomes more flexible when d is smaller; in other words, decrease in d induces larger contour length and smaller persistence length. As shown in Table 3, the alkyl-chain-associated core radius r_c for the star-like micelle of C16-PHEG was 1.1–1.2 nm and that for C18-PHEG was 1.3–1.4 nm. The value of $2r_c$ for C18 shows good consistency with the evaluated maximum value of d for C18-PHEG worm-like micelle, and in C16-PHEG, d was a littler smaller than $2r_c$. From these results, the assumption that C16- and C18-PHEG in W_{EG}=0.7 solution form worm-like cylindrical micelle can explain the experimentally obtained $M_{w,app}$ and $R_{g,app}$ consistently.

Finally, we need to point out the relationship between EG content in solvent and the structure of associates. R_h distribution curve indicated that the micelle is spherical shape when W_{EG}=0 and worm-like cylindrical when W_{EG}=0.7, and these two kinds of micelle coexisted when W_{EG} was in the range between these values. CD results revealed that f^H of PHEG increased with W_{EG}, and as reported by Ohta et al. [18], the increase in f^H induces a reduction in the PHEG molecular dimension. Therefore, the change of micellar shape from sphere to cylinder is accompanied with the decrease in the size of corona chain, and this tendency has similarity with the micelles of CiEj, i.e., the star-like micelle was formed when j=25 and worm-like cylinders were observed when $j \leq 8$. On the other hand, the association strength of alkyl chain decreases with the increase in W_{EG} because of the addition of more hydrophobic EG into water [14]. Reduction in the association strength will make the Cn-associated core be swollen by solvent, which also decreases the relative size of PHEG against Cn core. Therefore, in Cn-PHEG, the change of the micellar shape from sphere to cylinder might be explained by the decrease in the relative size of hydrophilic corona against the hydrophobic core with the increase in W_{EG}, caused by the above two effects.

Conclusions

Association behavior and structure of the associates for the one-end hydrophobically modified PHEG in selective solvent have been studied. The increase in α-helix content of PHEG with W_{EG} was recognized for all the Cn-PHEG. In C16- and C18-PHEG, formation of small micelles was suggested when W_{EG}=0. With the increase in W_{EG}, the appearance of a larger particle was revealed in R_h distribution curve, and unimodal distribution for this larger particle was observed when W_{EG}=0.7. In aqueous solution of C14-PHEG, formation of the small micelles with $R_{h,app}$~7 nm was also observed; however, increase in solubility of C14 chain without forming distinct micelles was suggested when W_{EG}>0.4. C12-PHEG did not reveal any distinct micellization behavior, probably because hydrophobicity of C12 chain attached at the terminal of PHEG with M_n~10,000 was too weak to form associated micelles.

In the small micelles of C14-, C16-, and C18-PHEG in aqueous solutions, the association number and radius of gyration were reasonably explained with assuming star-like spherical micelles with Cn core and PHEG corona. On the other hand, worm-like cylindrical micelles was suggested for the larger associates of C16- and C18-PHEG in W_{EG}=0.7 solutions to explain the observed $M_{w,app}$ and $R_{g,app}$ values. This structure change of the associates with the increase in W_{EG} was explained by the increase in f^H as well as the decrease in the association strength of Cn, both of which reduce the relative size of PHEG corona against Cn core.

Acknowledgments We would like to acknowledge the financial support by grant-in-aid for Scientific Research from the Japan Society for the Promotion of Science (No. 15550105).

References

1. Corkill JM, Walker T (1972) J Colloid Interface Sci 39:621
2. Brown W, Johnsen R, Stilbs P, Lindman B (1983) J Phys Chem 87:4548
3. Kato T, Seimiya T (1986) J Phys Chem 90:3159
4. Imae T (1988) J Phys Chem 92:5721
5. Yoshimura S, Shirai S, Einaga Y (2004) J Phys Chem B 108:15477
6. Imanishi K, Einaga Y (2005) J Phys Chem B 109:7574
7. Hamada N, Einaga Y (2005) J Phys Chem B 109:6990
8. Einaga Y, Kusumoto A, Noda A (2005) Polym J 37:368
9. Shirai S, Einaga Y (2005) Polym J 37:913
10. Einaga Y, Inaba Y, Syakado M (2006) Polym J 38:64
11. Yamazaki R, Inomata K, Nose T (2001) Kobunshi Ronbunshu 58:286
12. Yamazaki R, Inomata K, Nose T (2002) Polymer 43:3647
13. Sato T (2004) Langmuir 20:1095
14. Inomata K, Kasuya M, Sugimoto H, Nakanishi E (2005) Polymer 46:10035
15. Lotan N, Yaron A, Berger A (1966) Biopolymers 4:365
16. Adler AJ, Hoving R, Potter J, Wells M, Fasman GD (1968) J Am Chem Soc 90:4736
17. Miyake M, Akita S, Teramoto A, Norisuye T, Fujita H (1974) Biopolymers 13:1173
18. Ohta T, Norisuye T, Teramoto A, Fujita H (1976) Polym J 8:281
19. Inomata K, Itoh M, Nakanishi E (2005) Polym J 37:404
20. Gallot B, Hassan HH (1989) ACS Symp Ser 384:116
21. Cho CS, Nah JW, Jeong YI, Cheon JB, Asayama S, Ise H, Akaike T (1999) Polymer 40:6769
22. Tang D, Lin J, Lin S, Zhang S, Chen T, Tian X (2004) Macromol Rapid Commun 25:1241
23. Rodriguez-Hernández J, Lecommandoux S (2005) J Am Chem Soc 127:2026
24. Bae Y, Cabral H, Kataoka K (2006) In: Lazzari M, Liu G, Lecommandoux (eds) Block copolymer in nanoscience. Wiley, Weinheim, pp 73
25. Lecommandoux S, Klok HA, Schlaad H (2006) In: Lazzari M, Liu G, Lecommandoux (eds) Block copolymer in nanoscience. Wiley, Weinheim, pp 117
26. Sugimoto H, Nakanishi E, Hanai T, Yasumura T, Inomata K (2004) Polym Int 53:972
27. Daly WH, Poche D (1988) Tetrahedron Lett 29:5859
28. De Marre A, Soyez H, Schacht E, Pytela J (1994) Polymer 35:2443
29. Itakura M, Inomata K, Nose T (2001) Polymer 42:9261
30. Tsierkezos NG, Molinou IE (1998) J Chem Eng Data 43:989
31. Adler AJ, Hoving R, Potter J, Wells M, Fasman GD (1968) J Am Chem Soc 90:4736
32. Oka M, Hayashi T, Nakajima A (1985) Polym J 17:621
33. Fukumine Y, Inomata K, Takano A, Nose T (2000) Polymer 41:5367
34. Kanao M, Matsuda Y, Sato T (2003) Macromolecules 36:2093
35. Allison SA, Sorlie SS, Pecora R (1990) Macromolecules 23:1110
36. Iyama K, Nose T (1998) Polymer 39:651